IEEE Access
Multidisciplinary | Rapid Review | Open Access Journal

Received January 1, 2020, accepted January 12, 2020, date of publication January 24, 2020, date of current version February 5, 2020.

Digital Object Identifier 10.1109/ACCESS.2020.2969207

A Robust Guiding Torque Control Method for Automatic Steering Using LMI Algorithm

GUANGTONG BAI [1], CHUNJIANG BAO [1], JIAN WU [1], DEXI WU [1], JUNDA ZHANG [1], AND XIANGKUN HE [2]

[1] School of Mechanical and Automotive Engineering, Liaocheng University, Liaocheng 252059, China
[2] Noah's Ark Lab, Huawei Technologies, Beijing 100085, China

Corresponding author: Chunjiang Bao (baochunjiang@lcu.edu.cn)

This work was supported in part by the Key Research and Development Plan of Shandong Province, China, under Grant 2019GGX104047.

ABSTRACT The existing path tracking methods usually neglect the effect of the drivers on the steering control. This paper proposes a robust steering control method of human-machine steering torque superposition based on linear matrix inequality (LMI) algorithm. First, the model for solving steering superposition torque introduces the steering system and steering resistance torque model in addition to the vehicle model, which increases the nonlinearity and uncertainty of system, and the human in torque superposition control also increases the external interferences. Therefore, this paper proposes a LMI robust control algorithm to reduce the external interference and the influence of uncertain factors on the system and improve the tracking performance of system, by use of Lyapunov stability theory and Schur complement property to convert the region pole assignment and robust control constraint conditions into LMI convex optimization problem. The next, the nonlinear vehicle dynamics solving model including Fiala tire model, steering column model is established; the nonlinear tire model is linearized by use of affine function, and the steering superposition control law is solved by use of LMI. Then, the union CarSim and Simulink simulation is conducted under different situations to verify the robustness and control performance of control system. Finally, through establishing the hardware-in-the-loop experiment table based on LabVIEW-RT, the effectiveness of control strategy is verified. The test results show that the method solves the model uncertainty and the robustness decrement problem resulting from human intervention, ensuring a good tracking performance, and a stable system at the same time.

INDEX TERMS Steering system, intelligent vehicle, LMI, human-machine co-driving.

I. INTRODUCTION

With the rapid development of modern automobile technology, the unmanned vehicles will gradually achieve industrialization, the pilotless automobile has gradually become the hot topics studied by many scholars around the world [1]–[3]. Current unmanned driving is controlled usually by steering wheel angle [4], [5], often the steering intervention cannot be realized by a driver, thus completely separating the driver from autopilot control, easily causing the adverse effects such as "situational awareness" decreasing [6]–[8]. In order to solve the problem of the driver away from the control, this paper puts forward a kind of control method based on the steering torque input for the human-machine co-driving.

The associate editor coordinating the review of this manuscript and approving it for publication was Xiaoli Luan.

A lot of control methods are used for path tracking control research by predecessors, and have achieved a good control effect. In order to obtain the accuracy of path tracking under automatic driving, Marino *et al.* [9] use a nested PID steering control algorithm, through measuring by use of gyroscope etc., then the target path and road centerline deviation is used as a control input of controller, obtaining a better tracking effect. Zhang *et al.* [10] optimized the optimal PID controller parameters through ISE, IAE, ITAE, ITSE and other performance index, and obtained satisfactory dynamic and static performance. Vehicle dynamics model is established according to the vehicle parameters, and a steering system model is established based on least square method by Han *et al.* [11], and then the neural network PID controller for the dynamic model and the steering system model is established, this controller has a better real-time.

However, the parameter adjustment based on PID control algorithm usually uses the method of trial and error, and lack of self-adaptability. According to the finite preview optimal control method, Kang *et al.* [12] have designed the linear quadratic regulator (LQR) control system to realize the vehicle lateral control, and the path tracking effect is verified by real vehicle. Yakub and Mori [13] have linearized the nonlinear tire model, by use of the model predictive control (MPC), testing the path tracking performance at changing forward speed and road surface, the result of simulation shows that the controller will helpful to keep the vehicle stability. A multi-point preview driver model is combined with the linear quadratic optimal control (LQR) as the foundation [14], a steering control strategy is derived from Receding Horizon method, and achieving a good tracking effect.

The above control strategy belongs to a typical control method based on accurate model, its control effect is directly affected by the precision of model, a model has uncertainty in the actual application, so the robust control strategy for the path tracking problem is put forward. Hu *et al.* [15] proposes a robust H_∞ output feedback control method, the controller has the stronger robustness for the tire side cornering stiffness, yaw rate and surface curvature. He *et al.* [16] have proposed a robust control algorithm based on the linear matrix inequality (LMI), this method can keep a path tracking ability and stability under an uncertain external disturbance.

All of the above research strategy can solve the problem of path tracking well, but all of them are based on the steering wheel angle as a single input to control, thus a very precise angle calculation must be required, and the steering wheel is locked when working, leading to the driver can't intervene, when necessary, so that the driver will feel too nervous in the real driving. And it is humans machine co-driving at present and for some time to come, rather than completely unmanned. In order to solve this problem, Yang *et al.* [17] have proposed a path tracking control method of linear time-varying system based on model predictive control, the nonlinear vehicle dynamics model is established, the steering wheel torque is used as the control variable of system, realizing the function of human-machine co-driving.

But this method cannot solve the problem of road surface disturbance and sensor noise etc., the system can't have very good robustness [18], [19]. Therefore, main contributions of the paper are as follows:

1) The steering wheel torque is used as the control variable of system, the function of human-machine co-driving is introduced in this paper.

2). The robust human machine controller based on LMI is established, and solve the robustness problem about road surface disturbance and sensor noise.

The nonlinear fiala tire model is applied in this paper, local linear is conducted according to affine function, and then combining to the vehicle dynamics model. The second part of this paper is to establish mathematical model, mainly including steering column model, vehicle dynamics model; the third part mainly introduces the robust control algorithm based on LMI; the fourth part is the results of simulation; the fifth part is the result of experiment; the sixth part is summary.

II. ESTABLISHING MATHEMATICAL MODEL

A. STEERING SYSTEM DYNAMATICS MODEL

Steering system is shown in Fig. 1, it is a system for motor torque as a single input variable.

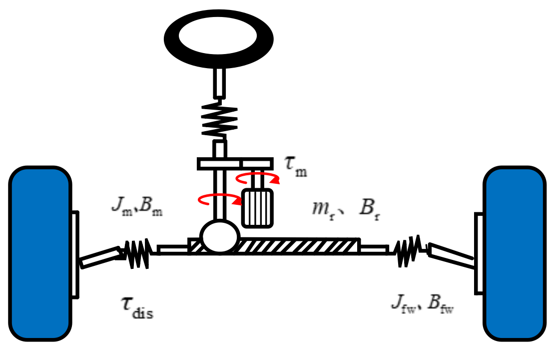

FIGURE 1. Steering system configuration.

The motor speed ratio and steering gear ratio are N_m and N_s respectively. To facilitate the combined with vehicle dynamics model, all the applied forces in steering system are equivalent to the steering knuckle, so equation (1) can be derived.

$$J_{eq}\ddot{\delta} + B_{eq}\dot{\delta} + \tau_{dis} + \tau_f \operatorname{sign}(\dot{\delta}) = N_s N_m \tau_m \tag{1}$$

where, τ_m is motor torque, τ_{dis} is the steering resistance torque of ground surface to tire, τ_f is the friction torque of steering system, δ is steering wheel angle. Inertia J_eq and damping B_eq in the steering knuckle of steering system is respectively:

$$\begin{aligned} J_{eq} &= J_{fw} + (N_m N_s)^2 J_m + N_s^2 (J_c + m_r r_p^2) \\ B_{eq} &= B_{fw} + (N_m N_s)^2 B_m + N_s^2 (B_c + B_r r_p^2) \end{aligned}$$

By using $\boldsymbol{x}_1 = \begin{bmatrix} \delta & \dot{\delta} \end{bmatrix}$ as state variable, convert (1) into state space model (2):

$$\begin{aligned} \dot{\boldsymbol{x}}_1 &= \boldsymbol{A}_1 \boldsymbol{x}_1 + \boldsymbol{B}_1 \boldsymbol{\tau}_\mathrm{m} + \boldsymbol{N}_1 \boldsymbol{w}_1 \\ \boldsymbol{y}_1 &= \boldsymbol{C}_1 \boldsymbol{x}_1 \end{aligned} \tag{2}$$

where

$$\boldsymbol{A}_1 = \begin{bmatrix} 0 & 1 \\ 0 & -\dfrac{B_{eq}}{J_{eq}} \end{bmatrix} \quad \boldsymbol{B}_1 = \begin{bmatrix} 0 \\ \dfrac{N_m N_s}{J_{eq}} \end{bmatrix} \quad \boldsymbol{N}_1 = \begin{bmatrix} 0 \\ -\dfrac{1}{J_{eq}} \end{bmatrix}$$

$$\boldsymbol{C}_1 = \begin{bmatrix} 1 & 0 \end{bmatrix} \qquad w_1 = \tau_{dis} + \tau_f \operatorname{sign}(\dot{\delta})$$

Equation 2 expresses the relationship between the motor torque τ_m and the steering wheel angle. Where, steering resisting moment τ_{dis} and steering system friction torque τ_f are added into the system in the form of external disturbance.

B. VEHICLE DYNAMIC MODEL

This section describes the combination of tire model with vehicle two dof model, nonlinear tire can be described as Fiala tire model (3) [20].

$$F_y = \begin{cases} -\mu F_z \left[1 - \left(1 - \dfrac{C_\alpha |\tan\alpha|}{3\mu F_z}\right)^3\right] \operatorname{sgn}(\alpha), & |\alpha| < \alpha_{sl} \\ -\mu F_z \operatorname{sgn}(\alpha), & |\alpha| \geq \alpha_{sl} \end{cases} \tag{3}$$

where, F_z represents the vertical force applied on the automobile, μ is the friction factor of ground, α is side slip angle, C_α is cornering stiffness.

In order to simplify the calculation complexity, the local linearization of nonlinear Fiala tire model is conducted, as shown in Fig. 2. The process can be described as: Fiala tire model is divided into the infinite sub-segments, thus each segment is approximate to a straight line, the slope of any point on each straight line can be considered with the same value, the value is the tire side angle stiffness. Then supposing that the side angle of the initial point on the straight line is α_0, the corresponding cornering force is F_{y0}, then its cornering force at other location on the straight line can be described the following affine function:

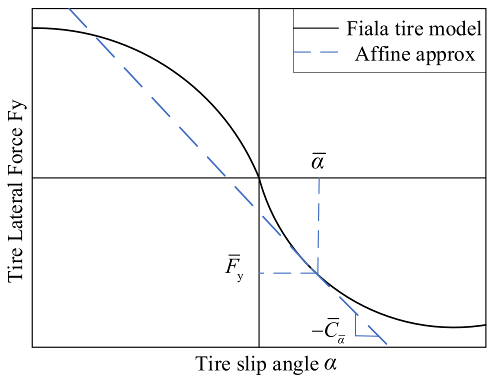

FIGURE 2. Linearization of tire model.

Where, if the sideslip angle of front and rear tire is α_{f0}, α_{r0}, the tire cornering stiffness corresponds to C_{f0}, C_{r0}, the lateral force corresponding to the front and rear tire is respectively F_{yf}, F_{yr}.

$$\begin{aligned} F_{yf}(\alpha_f) &= F_{yf0} + C_{f0}(\alpha_f - \alpha_{f0}) \\ F_{yr}(\alpha_r) &= F_{yr0} + C_{r0}(\alpha_r - \alpha_{r0}) \end{aligned} \tag{4}$$

Assuming that the vehicle's longitudinal speed is constant, thus a nonlinear two degrees of freedom vehicle dynamics model [21] is shown in Fig. 3, so that:

$$\begin{cases} \dot{v}_y = \dfrac{1}{m}\left[F_{yf}(\alpha_f) + F_{yr}(\alpha_f)\right] - v_x\dot{\psi} \\ \ddot{\psi} = \dfrac{1}{I_z}\left[aF_{yf}(\alpha_f) - bF_{yr}(\alpha_f)\right] \end{cases} \tag{5}$$

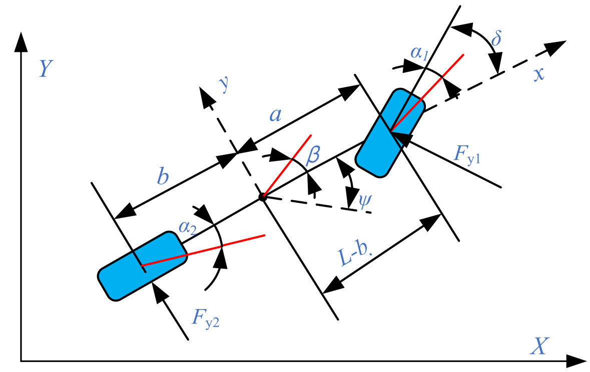

FIGURE 3. Automobile dynamics model.

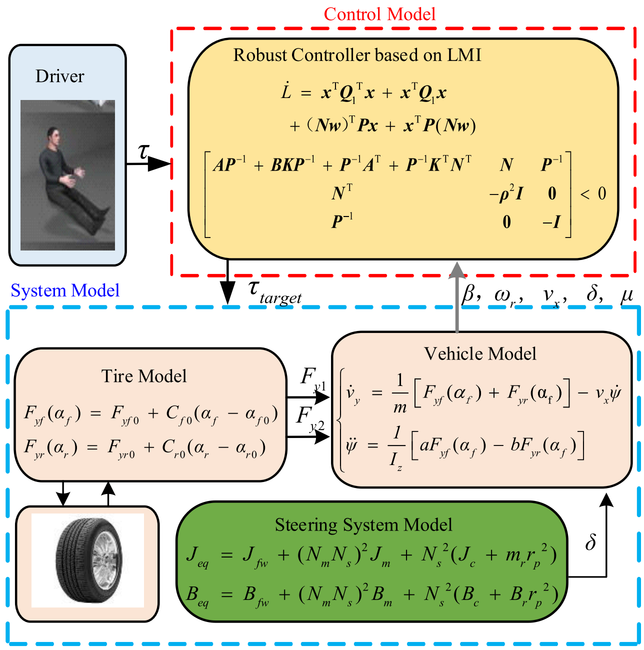

FIGURE 4. Path tracking control strategy.

where, m is quality of automobile, v_x is speed of of automobile, ω_r is yaw velocity of automobile, I_z is the rotational inertia of automobile along the y-axis direction, β is sideslip angle of automobile, a and b are respectively the distance from the automobile mass center to the front and rear axle, F_{y1}, F_{y2} represent respectively the cornering force applied on automobile front and rear wheels. Sideslip angle α_f, α_r of front and rear wheels are respectively:

$$\begin{aligned} \alpha_f &= \frac{v_y + a\dot{\psi}}{v_x} - \delta \\ \alpha_r &= \frac{v_y - b\dot{\psi}}{v_x} \end{aligned} \tag{6}$$

By combining the equation (4), (5) and (6), and converting into matrix form, the automobile two degree of freedom model merging tire model (8) can be derived, the model can represent the dynamical response of lateral automobile movement to the input steering wheel angle.

$$\begin{aligned} \dot{x}_2 &= A_2x_2 + B_2u_2 + N_2w_2 \\ y_2 &= C_2x_2 \end{aligned} \tag{7}$$

where, status variable $\boldsymbol{x}_2 = \begin{bmatrix} Y & v_y & \psi & \dot{\psi} \end{bmatrix}^T$

$$\boldsymbol{y}_2 = \begin{bmatrix} Y & \psi \end{bmatrix}^T$$

$$\boldsymbol{A}_2 = \begin{bmatrix} 0 & 1 & v_x & 0 \\ 0 & \dfrac{C_{f0}+C_{r0}}{mv_x} & 0 & \dfrac{aC_{f0}-bC_{r0}}{mv_x} \\ 0 & 0 & 0 & 1 \\ 0 & \dfrac{aC_{f0}-bC_{r0}}{I_zv_x} & 0 & \dfrac{a^2C_{f0}-b^2C_{r0}}{I_zv_x} \end{bmatrix}$$

$$\boldsymbol{B}_2 = \begin{bmatrix} 0 \\ \dfrac{-C_f}{m} \\ 0 \\ \dfrac{-aC_f}{I_z} \end{bmatrix} \quad \boldsymbol{N}_2 = \begin{bmatrix} 0 & 0 \\ 1 & 0 \\ 0 & 0 \\ 0 & 1 \end{bmatrix} \quad \boldsymbol{C}_2 = \begin{bmatrix} 1 & 0 & 0 & 0 \\ 0 & 0 & 1 & 0 \end{bmatrix}$$

$$\boldsymbol{w}_2^{\mathrm{T}} = \begin{bmatrix} \dfrac{F_{yf0}+F_{yr0}-C_{\alpha f0}\alpha_{f0}-C_{\alpha r0}\alpha_{r0}}{m} \\ \dfrac{aF_{yf0}-bF_{yr0}-aC_{\alpha f0}\alpha_{f0}+bC_{\alpha r0}\alpha_{r0}}{I_z} \end{bmatrix}$$

C. COMBINATION OF STEERING SYSTEM AND COMPLETE VEHICLE SYSTEM

By combining (2) and (7), a complete vehicle dynamic model (8) integrated into the steering system can be obtained.

$$\begin{aligned} &\dot{\boldsymbol{x}} = \boldsymbol{Ax} + \boldsymbol{Bu} + \boldsymbol{Nw} \\ &\boldsymbol{y} = \boldsymbol{x} \\ &\boldsymbol{A} = \begin{bmatrix} \boldsymbol{A}_1 & \boldsymbol{0} \\ \boldsymbol{B}_2\boldsymbol{C}_1 & \boldsymbol{A}_2 \end{bmatrix} \quad \boldsymbol{B} = \begin{bmatrix} \boldsymbol{B}_1 \\ \boldsymbol{0} \end{bmatrix} \quad \boldsymbol{N} = \begin{bmatrix} \boldsymbol{N}_1 & \boldsymbol{0} \\ \boldsymbol{0} & \boldsymbol{N}_2 \end{bmatrix} \\ &\boldsymbol{x} = \begin{bmatrix} \delta & \dot{\delta} & Y & v_y & \psi & \omega_r \end{bmatrix}^{\mathrm{T}} \quad \boldsymbol{w} = \begin{bmatrix} \boldsymbol{\tau}_{dis} & \boldsymbol{w}_2 \end{bmatrix}^{\mathrm{T}} \end{aligned} \tag{8}$$

III. ROBUST CONTROLLER DESIGN BASED ON LMI

The robust control law can be supposed to

$$\boldsymbol{u} = \boldsymbol{Kx} \tag{9}$$

K is the state feedback gain matrix Lyapunov function [22] is:

$$L = \boldsymbol{x}^{\mathrm{T}}\boldsymbol{Px} \tag{10}$$

where, P is positive definite matrix, thus according to (8) and (9), a derivation for (10) is:

$$\begin{aligned} \dot{L} &= \dot{\boldsymbol{x}}^{\mathrm{T}}\boldsymbol{Px} + \boldsymbol{x}^{\mathrm{T}}\boldsymbol{P}\dot{\boldsymbol{x}} \\ &= (\boldsymbol{Ax}+\boldsymbol{BKx}+\boldsymbol{Nw})^{\mathrm{T}}\boldsymbol{Px} + \boldsymbol{x}^{\mathrm{T}}\boldsymbol{P}(\boldsymbol{Ax}+\boldsymbol{BKx}+\boldsymbol{Nw}) \end{aligned} \tag{11}$$

Supposing

$$\boldsymbol{Q}_1 = \boldsymbol{P}(\boldsymbol{A}+\boldsymbol{BK}) \tag{12}$$

Thus

$$\dot{L} = \boldsymbol{x}^{\mathrm{T}}\boldsymbol{Q}_1^{\mathrm{T}}\boldsymbol{x} + \boldsymbol{x}^{\mathrm{T}}\boldsymbol{Q}_1\boldsymbol{x} + (\boldsymbol{Nw})^{\mathrm{T}}\boldsymbol{Px} + \boldsymbol{x}^{\mathrm{T}}\boldsymbol{P}(\boldsymbol{Nw}) \tag{13}$$

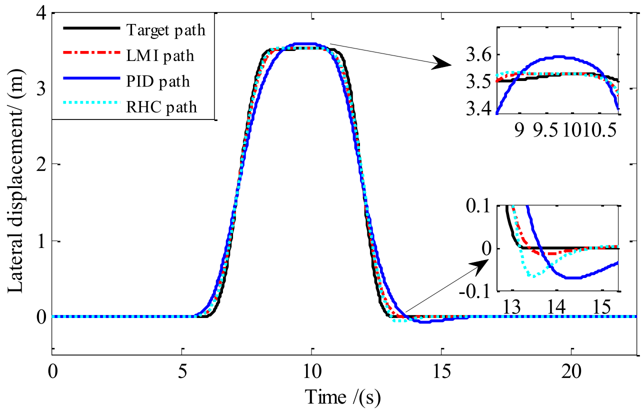

FIGURE 5. Tracking performance of simulation.

$$\begin{aligned} &\boldsymbol{x}^{\mathrm{T}}\boldsymbol{Q}_1^{\mathrm{T}}\boldsymbol{x} + \boldsymbol{x}^{\mathrm{T}}\boldsymbol{Q}_1\boldsymbol{x} = \boldsymbol{x}^{\mathrm{T}}\boldsymbol{Qx} = \begin{bmatrix} \boldsymbol{x}^{\mathrm{T}} & \boldsymbol{w}^{\mathrm{T}} \end{bmatrix} \begin{bmatrix} \boldsymbol{Q} & \boldsymbol{0} \\ \boldsymbol{0} & \boldsymbol{0} \end{bmatrix} \begin{bmatrix} \boldsymbol{x} \\ \boldsymbol{w} \end{bmatrix} \\ &(\boldsymbol{Nw})^{\mathrm{T}}\boldsymbol{Px} + \boldsymbol{x}^{\mathrm{T}}\boldsymbol{P}(\boldsymbol{Nw}) = \begin{bmatrix} \boldsymbol{x}^{\mathrm{T}} & \boldsymbol{w}^{\mathrm{T}} \end{bmatrix} \begin{bmatrix} \boldsymbol{0} & \boldsymbol{PN} \\ \boldsymbol{N}^{\mathrm{T}}\boldsymbol{P} & \boldsymbol{0} \end{bmatrix} \begin{bmatrix} \boldsymbol{x} \\ \boldsymbol{w} \end{bmatrix} \end{aligned} \tag{14}$$

Equation (15) can be derived from equation (13).

$$\dot{L} = \begin{bmatrix} \boldsymbol{x}^{\mathrm{T}} & \boldsymbol{w}^{\mathrm{T}} \end{bmatrix} \begin{bmatrix} \boldsymbol{Q} & \boldsymbol{PN} \\ \boldsymbol{N}^{\mathrm{T}}\boldsymbol{P} & \boldsymbol{0} \end{bmatrix} \begin{bmatrix} \boldsymbol{x} \\ \boldsymbol{w} \end{bmatrix} = \boldsymbol{\lambda}^{\mathrm{T}} \begin{bmatrix} \boldsymbol{Q} & \boldsymbol{PN} \\ \boldsymbol{N}^{\mathrm{T}}\boldsymbol{P} & \boldsymbol{0} \end{bmatrix} \boldsymbol{\lambda} \tag{15}$$

where

$$\boldsymbol{\lambda} = \begin{bmatrix} \boldsymbol{x}^{\mathrm{T}} \\ \boldsymbol{w}^{\mathrm{T}} \end{bmatrix}, \quad \boldsymbol{\lambda}^{\mathrm{T}} = \begin{bmatrix} \boldsymbol{x}^{\mathrm{T}} & \boldsymbol{w}^{\mathrm{T}} \end{bmatrix}$$

The selection of performance indicators is:

$$\int_0^t \boldsymbol{y}^{\mathrm{T}}\boldsymbol{y}\mathrm{d}t \le \rho^2 \int_0^t \boldsymbol{w}^{\mathrm{T}}\boldsymbol{w}\mathrm{d}t \tag{16}$$

According to the equation (9), can derive:

$$\begin{aligned} \boldsymbol{y}^{\mathrm{T}}\boldsymbol{y} - \rho^2\boldsymbol{w}^{\mathrm{T}}\boldsymbol{w} &= \boldsymbol{x}^{\mathrm{T}}\boldsymbol{x} - \rho^2\boldsymbol{w}^{\mathrm{T}}\boldsymbol{w} \\ &= \begin{bmatrix} \boldsymbol{x}^{\mathrm{T}} & \boldsymbol{w}^{\mathrm{T}} \end{bmatrix} \begin{bmatrix} \boldsymbol{I} & \boldsymbol{0} \\ \boldsymbol{0} & -\rho^2\boldsymbol{I} \end{bmatrix} \begin{bmatrix} \boldsymbol{x} \\ \boldsymbol{w} \end{bmatrix} \\ &= \boldsymbol{\lambda}^{\mathrm{T}} \begin{bmatrix} \boldsymbol{I} & \boldsymbol{0} \\ \boldsymbol{0} & -\rho^2\boldsymbol{I} \end{bmatrix} \boldsymbol{\lambda} \end{aligned} \tag{17}$$

According to (15) and (17), (18) can derived by adding two equation:

$$\dot{L} + \boldsymbol{y}^{\mathrm{T}}\boldsymbol{y} - \rho^2\boldsymbol{w}^{\mathrm{T}}\boldsymbol{w} = \boldsymbol{\lambda}^{\mathrm{T}} \begin{bmatrix} \boldsymbol{Q}+\boldsymbol{I} & \boldsymbol{PN} \\ \boldsymbol{N}^{\mathrm{T}}\boldsymbol{P} & -\rho^2\boldsymbol{I} \end{bmatrix} \boldsymbol{\lambda} \tag{18}$$

Supposing

$$\begin{bmatrix} \boldsymbol{Q}+\boldsymbol{I} & \boldsymbol{PN} \\ \boldsymbol{N}^{\mathrm{T}}\boldsymbol{P} & -\rho^2\boldsymbol{I} \end{bmatrix} < 0 \tag{19}$$

Thus

$$\dot{L} + \boldsymbol{y}^{\mathrm{T}}\boldsymbol{y} - \rho^2\boldsymbol{w}^{\mathrm{T}}\boldsymbol{w} \le 0 \tag{20}$$

By integrating (20), can derive:

$$\begin{aligned} L &\le \rho^2 \int_0^t \boldsymbol{w}^{\mathrm{T}}\boldsymbol{w}\mathrm{d}t - \int_0^t \boldsymbol{y}^{\mathrm{T}}\boldsymbol{y}\mathrm{d}t + L(0) \\ &\le \rho^2 \int_0^t \boldsymbol{w}^{\mathrm{T}}\boldsymbol{w}\mathrm{d}t + L(0) \end{aligned} \tag{21}$$

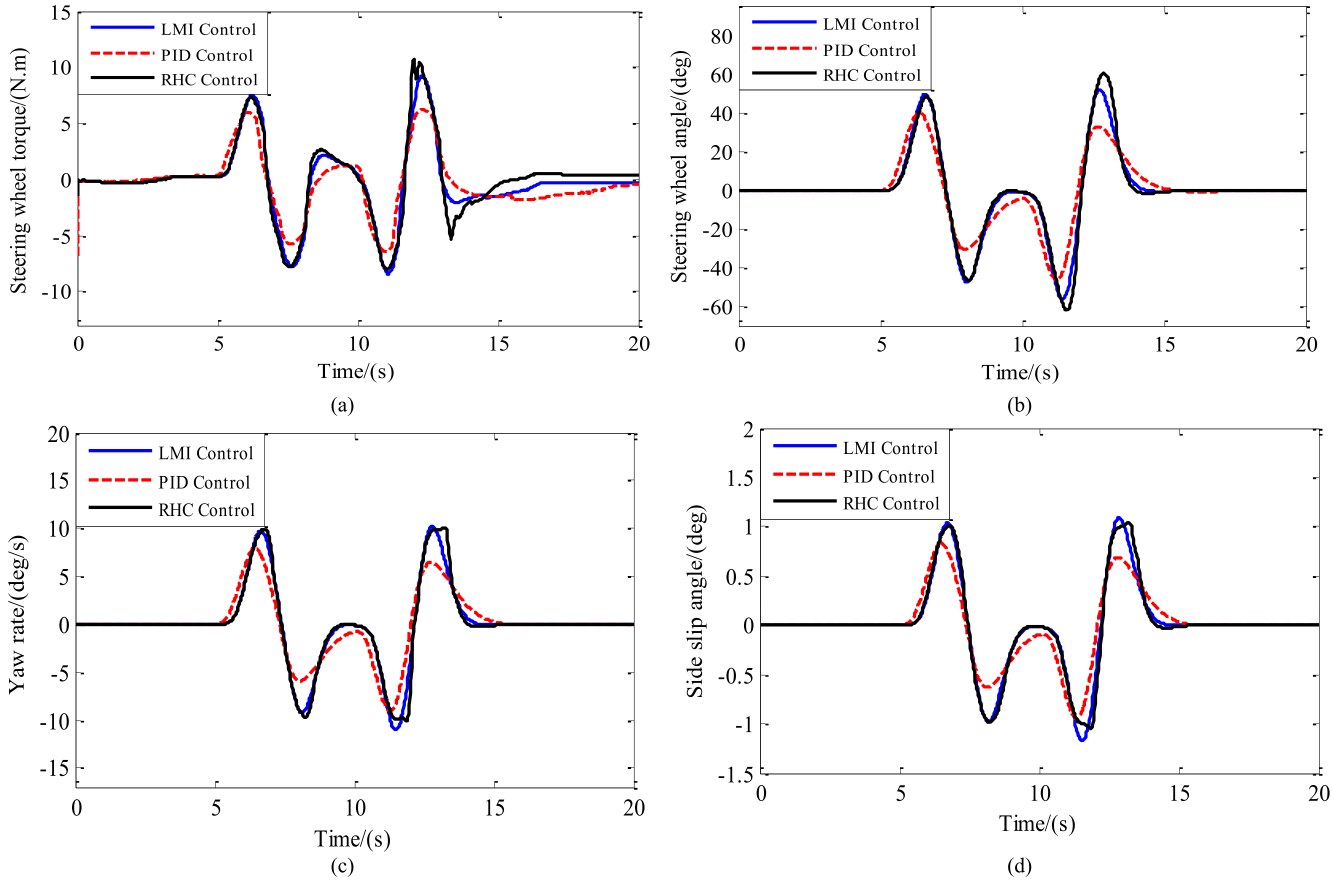

FIGURE 6. a) Steering wheel torque. b) Steering wheel angle. c) Yaw rate. d) Side slip angle.

By the equation (10) and (21), can derive:

$$\boldsymbol{P}_{\min}\|x\|^2 \leq \boldsymbol{x}^{\mathrm{T}}\boldsymbol{P}\boldsymbol{x} \leq \rho^2\int_0^t \boldsymbol{w}^{\mathrm{T}}\boldsymbol{w}\mathrm{d}t + L(0)$$

Thus

$$\|\boldsymbol{x}\|^2 \leq \frac{\rho^2\int_0^t \boldsymbol{w}^{\mathrm{T}}\boldsymbol{w}\mathrm{d}t + L(0)}{\boldsymbol{P}_{\min}} \tag{22}$$

Therefore, under the limited time domain and defined interference, the state of the system is bounded. However, the premise meeting the above situation is the establishment of (19). According to the Schur complement lemma, (19) can converted into:

$$\begin{bmatrix} \boldsymbol{Q} & \boldsymbol{PN} & \boldsymbol{I} \\ \boldsymbol{N}^{\mathrm{T}}\boldsymbol{P} & -\rho^2\boldsymbol{I} & 0 \\ \boldsymbol{I} & 0 & -\boldsymbol{I} \end{bmatrix} < 0 \tag{23}$$

According to the equation (13), (14), (23) can be turned into (24):

$$\begin{bmatrix} \boldsymbol{PA}+\boldsymbol{PBK}+\boldsymbol{A}^{\mathrm{T}}\boldsymbol{P}+\boldsymbol{K}^{\mathrm{T}}\boldsymbol{B}^{\mathrm{T}}\boldsymbol{P} & \boldsymbol{PN} & \boldsymbol{I} \\ \boldsymbol{N}^{\mathrm{T}}\boldsymbol{P} & -\rho^2\boldsymbol{I} & 0 \\ \boldsymbol{I} & 0 & -\boldsymbol{I} \end{bmatrix} < 0 \tag{24}$$

Supposing matrix $\boldsymbol{Z} = \begin{bmatrix} \boldsymbol{P}^{-1} & 0 & 0 \\ 0 & \boldsymbol{I} & 0 \\ 0 & 0 & \boldsymbol{I} \end{bmatrix}$ both sides in the matrix is multiplied by $\boldsymbol{Z}$, can derive:

$$\begin{bmatrix} \boldsymbol{AP}^{-1}+\boldsymbol{BKP}^{-1}+\boldsymbol{P}^{-1}\boldsymbol{A}^{\mathrm{T}}+\boldsymbol{P}^{-1}\boldsymbol{K}^{\mathrm{T}}\boldsymbol{N}^{\mathrm{T}} & \boldsymbol{N} & \boldsymbol{P}^{-1} \\ \boldsymbol{N}^{\mathrm{T}} & -\rho^2\boldsymbol{I} & 0 \\ \boldsymbol{P}^{-1} & 0 & -\boldsymbol{I} \end{bmatrix} < 0 \tag{25}$$

because of the positive definite matrix $\boldsymbol{P}$, so that:

$$\boldsymbol{P} > 0 \tag{26}$$

Combining the equation (25) and (26), the gain matrix $\boldsymbol{K}$ can solved by using MATLAB LMI toolbox.

IV. SIMULATION AND RESULT ANALYSIS

In this section, the target path is set as a double lane change, the mathematical model built through the Matlab/Simulink is simulated jointly with CarSim, the gain matrix K solved by the above part is substituted into a combined simulation model. In simulation model CarSim, the ground adhesion coefficient is set as $\mu = 1$, the speed $v_x = 40$km/h. In addition, in order to highlight better the advantages of LMI control algorithm, this paper also sets up the control algorithm based on PID and Receding Horizon Control (RHC) for contrast, its path tracking effect is shown in Fig. 5.

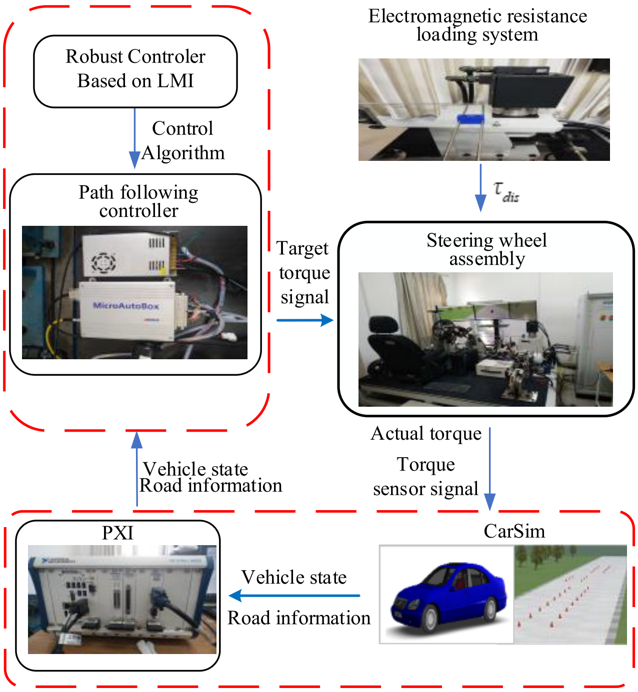

FIGURE 7. Structure diagram for hardware-in-the-loop test.

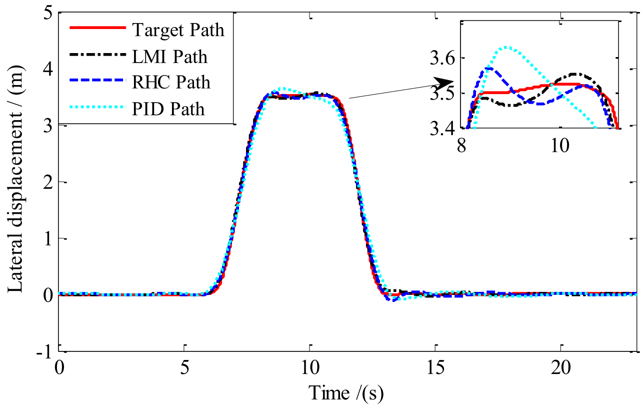

FIGURE 8. Tracking performance of experiment.

As can be seen from Fig. 5, the control algorithm based on PID and the robust control strategy based on LMI can track very well the target path, but the overshoot for the control algorithm based on PID is larger in process of 100-120 m and 100-180 m, and path deviation is larger in the process of 60-170 meters. However, the overall jitter for the robust control algorithm based on LMI is smaller, without too large overshoot, the overall tracking effect is better.

The steering wheel torque and angle based on three algorithm are shown in Fig. 6a and Fig. 6b, as shown in the figure, the steering wheel torque and angle based on PID, RHC and LMI algorithm can turn very well with the change of path. The turning angle for the path tracking based on PID control is smaller, the torque amplitude under RHC control is enough, but its overall vibration is larger, but the response under the LMI control can not only ensure enough turning angle but also more gently, the effect is better.

Fig. 6c and Fig. 6d are the contrast figure for the horizontal pendulum angular velocity and mass center side-slip angle under three algorithms. From the figure, it can be seen that the horizontal pendulum angular velocity and mass center side-slip angle for the path tracking under PID control reach to stable for a long time. This two parameters under RHC and LMI control reach to stable fast, but before reaching the steady state, the response speed of RHC is slower than the response speed under the LMI control, and tracking accuracy is poorer.

V. TEST OF HARDWARE-IN-THE-LOOP

A. TEST OF PATH TRACKING BASED ON TORQUE CONTROL

Through constructing the hardware-in-the-loop experiment bench based on LabVIEW RT, the designed path tracking robust control algorithm is verified. Hardware-in-the-loop experiment bench consists of PXI, dSPACE, steering rack, etc. Among them, the control procedures are embedded into dSPACE real time system by building of Simulink, CarSim including vehicle dynamics model and road information are embedded into PXI real time system by LabVIEW, the steering resistance torque is loaded through the servo motor, the communication between components is realized through analog signals or CAN signals.

Fig. 8 is the data collected by test, the experiment set speed is 40 km/h, roads with double lane change, ground adhesion μ value is 1. It can be seen from the Fig. 8, three kinds of control algorithm can better track the target path, but the tracking effect under the LMI control algorithm with respect to the other two has faster response, smaller overshoot, more smooth curve, the overall tracking effect is the best.

Fig. 9a and Fig. 9b is the angle and torque condition under all kinds of control algorithm collected by test, it can be seen from the figure, all the three kinds of control algorithm can calculate the target torque according to the requirements of path, which applies to the motor and generates the corresponding steering wheel angle. But when changing lanes in double lane change, the steering wheel torque under the LMI control with respect to the other two control is bigger, the response is faster, it shows that vehicles can more quickly and more stably avoid the obstacles ahead under emergency cases, and it can effectively improve the operation and safety performance of automobile.

Fig. 9c is the current data of steering system execution motor collected by test, it can be seen from the figure, during 14∼20 s, the motor current curve under the PID control

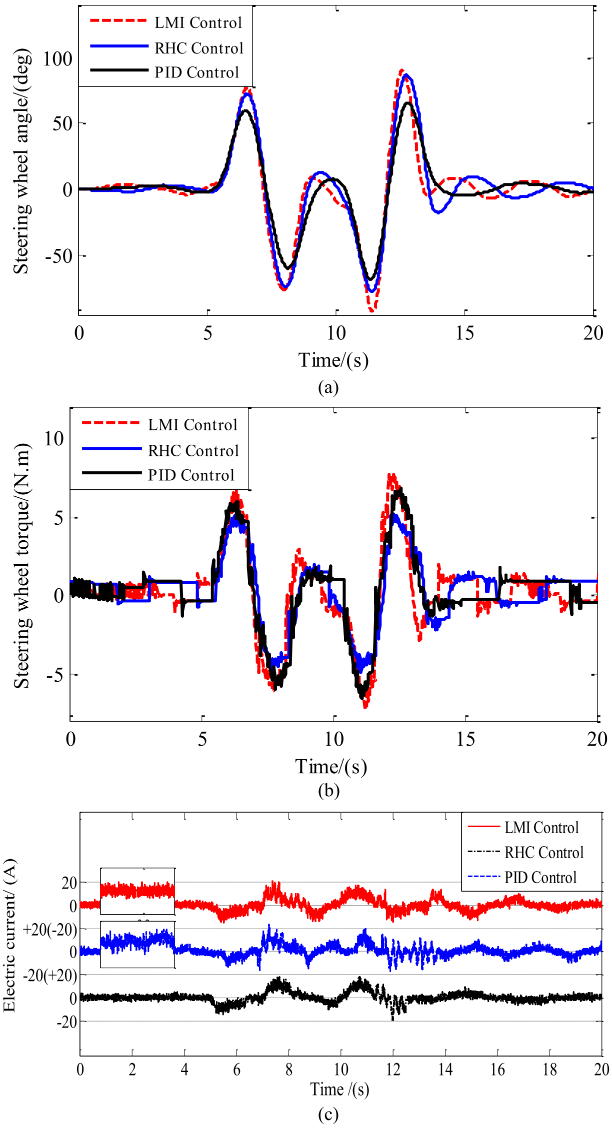

FIGURE 9. a) Steering wheel angle. b) Steering wheel torque. c) Electric current.

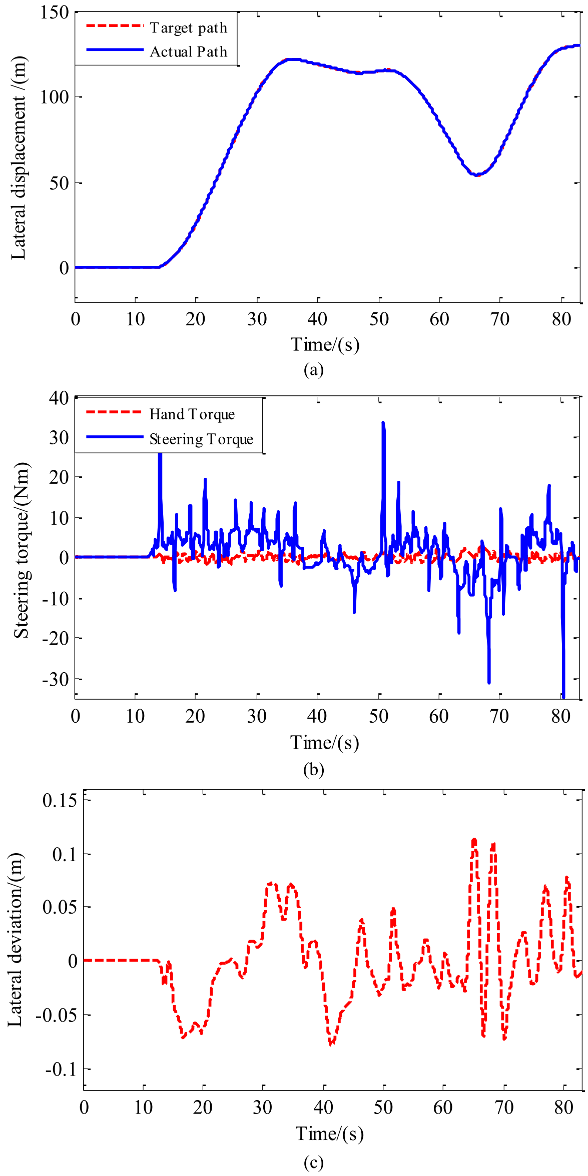

FIGURE 10. a) Tracking performance of co-driving. b) Steering torque of co-driving. c) Lateral deviation of co-driving.

tends to level, it shows that the control algorithm cannot well make the quick vehicle action according to path. The motor current controlled by RHC and LMI can allow the vehicle to move more quickly depending on the path, but by the comparison between the two, under RHC control, the noise of motor current has some fluctuation; but under LMI control, the current is more stable, this shows that the system ability against interference under LMI control is stronger, the system robust performance is better.

B. TEST OF HUMAN-MACHINE CO-DRIVINE

This paper verifies the performance of human-machine co-driving system by selecting a part of serpentine route, the set condition is as follows: the speed is 40km/h, the front preview distance is 15 m, a control of the vehicle is realized together through the professional drivers and controllers, the tested serpentine road and tracking effect are shown in Fig.10a.

Fig. 10b is the hand torque and steering shaft total torque collected under the path tracking control based on torque control, based on the path tracking in control of torque control, the driver can be involved in controlling the vehicle steering system, and the robust control algorithm based on LMI can well ensure the stability of vehicle. It can be seen from Fig. 10c, for the serpentine path tracking control of human-machine co-participation, the tracking error is within ± 0.11 m, the overall tracking effect is ideal.

VI. SUMMARY

This paper designs a path tracking controller for the steering torque input of robust control algorithm based on LMI, and it is verified by relevant test. Main works in this paper can be divided into the following several parts:

A. Setting up the steering column model and nonlinear two degree of freedom vehicle model, considering such problems as interference and uncertainty.

B. The effectiveness of the control algorithm has been verified through the simulation and hardware-in-the-loop test platform. Simulation and test results show that the LMI robust controller based on torque control can realize the path tracking under human-machine co-driving, and can ensure stability and robust performance of the system.

REFERENCES

[1] E. Coelingh, J. Nilsson, and J. Buffum, "Driving tests for self-driving cars," *IEEE Spectr.*, vol. 55, no. 3, pp. 40–45, Mar. 2018.

[2] B. Brown, "The social life of autonomous cars," *Computer*, vol. 50, no. 2, pp. 92–96, Feb. 2017.

[3] S. Karnouskos, "Self-driving car acceptance and the role of ethics," *IEEE Trans. Eng. Manag.*, to be published.

[4] M. Park, S. Lee, and W. Han, "Development of steeing control system for autonomous vehicle using geometry based path tracking algorithm," *Etri J.*, vol. 37, no. 3, pp. 617–625, 2015.

[5] Y. Feng, R. Du, and Y. Xu, "Steering angle balance control method for rider-less bicycle based on ADAMS," in *Proc. Int. Conf. Intell. Transp.* Springer, 2016, pp. 15–31.

[6] D. Tan, W. Chen, H. Wang, and Z. Gao, "Shared control for lane departure prevention based on the safe envelope of steering wheel angle," *Control Eng. Pract.*, vol. 64, pp. 15–26, Jul. 2017.

[7] X. Ji, J. Wu, Y. Zhao, Y. Liu, and X. Zhao, "A new robust control method for active front steering considering the intention of the driver," *Proc. Inst. Mech. Eng., D, J. Automobile Eng.*, vol. 229, no. 4, pp. 518–531, Mar. 2015.

[8] J. Wu, Y. Zhao, X. Ji, Y. Liu, and L. Zhang, "Generalized internal model robust control for active front steering intervention," *Chin. J. Mech. Eng.*, vol. 28, no. 2, pp. 285–293, Mar. 2015.

[9] R. Marino, S. Scalzi, and M. Netto, "Nested PID steering control for lane keeping in autonomous vehicles," *Control Eng. Pract.*, vol. 19, no. 12, pp. 1459–1467, Dec. 2011.

[10] M. Zhang, X. Lin, Y. Ding, W. Yin, and Q. Yan, "Design of path following controllers based on performance index for agricultural vehicle," *Trans. Chin. Soc. Agricult. Eng.*, vol. 28, no. 9, pp. 40–46, 2012.

[11] G. Han, W. Fu, W. Wang, and Z. Wu, "The Lateral tracking control for the intelligent vehicle based on adaptive PID neural network," *Sensors*, vol. 17, no. 6, p. 1244, May 2017.

[12] J. Kang, R. Y. Hindiyeh, S.-W. Moon, J. C. Gerdes, and K. Yi, "Design and testing of a controller for autonomous vehicle path tracking using GPS/INS sensors," *IFAC Proc. Vol.*, vol. 41, no. 2, pp. 2093–2098, 2008.

[13] F. Yakub and Y. Mori, "Comparative study of autonomous path-following vehicle control via model predictive control and linear quadratic control," *Proc. Inst. Mech. Eng., D, J. Automobile Eng.*, vol. 229, no. 12, pp. 1695–1714, Oct. 2015.

[14] J. Wu, S. Cheng, and B. Liu, "A human-machine-cooperative-driving controller based on AFS and DYC for vehicle dynamic stability," *Energies*, no. 10, vol. 11, pp. 1737–1747, 2017.

[15] H. Jing, C. Hu, F. Yan, M. Chadli, R. Wang, and N. Chen, "Robust H_∞ output-feedback control for path following of autonomous ground vehicles," in *Proc. 54th IEEE Conf. Decision Control (CDC)*, vol. 70, Dec. 2015, pp. 1515–1520.

[16] X. He, Y. Liu, K. Yang, J. Wu, and X. Ji, "Robust coordination control of AFS and ARS for autonomous vehicle path tracking and stability," in *Proc. IEEE Int. Conf. Mechatronics Autom. (ICMA)*, Aug. 2018, pp. 924–929.

[17] K. Yang, Y. Liu, Y. Liu, X. He, and X. Ji, "A linear time-varying MPC method for vehicle path-following assistance based on steering torque," in *Proc. 43rd Annu. Conf. IEEE Ind. Electron. Soc.*, Oct. 2017, pp. 4559–4564.

[18] A. Mitov, T. Slavov, J. Kralev, and I. Angelov, "Comparison of robust stability for electrohydraulic steering control system based on LQG and $H-_\infty$ Controller," in *Proc. 42nd Int. Conf. Telecommun. Signal Process. (TSP)*, Jul. 2019, pp. 712–715.

[19] J. Wu, X. Wang, and L. Li, "Hierarchical control strategy with battery aging consideration for hybrid electric vehicle regenerative braking control," *Energy*, vol. 145, pp. 301–312, 2018.

[20] B. Igo, "MF-tire/MF-swift parameters and estimation methods," in *Tire and Vehicle Dynamics*. 2012, pp. 613–625.

[21] Z. Yu, *The Theory of Automobiles*, 5th ed. Beijing, China: Mechanical industry Press, 2009.

[22] S. K. Das, M. Rahman, S. K. Paul, M. Armin, P. N. Roy, and N. Paul, "High-performance robust controller design of plug-in hybrid electric vehicle for frequency regulation of smart grid using linear matrix inequality approach," *IEEE Access*, vol. 7, pp. 116911–116924, 2019.

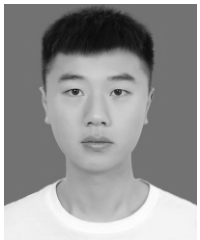

GUANGTONG BAI received the B.S. degree in vehicle engineering from Liaocheng University, Shandong, China, in 2018, where he is currently pursuing the M.S. degree in vehicle engineering. His research interests include intelligent vehicle dynamics and control, and electric vehicle chassis coordinated control.

CHUNJIANG BAO received the Ph.D. degree in mechanical engineering from Shenyang Agricultural University, China, in 2002. He is currently a Professor and the Dean of the School of Mechanical and Automotive Engineering, Liaocheng University, Shandong, China. He is the Executive Director of the Shandong Automotive Engineering Society. His research interests include systems integrated control of intelligent vehicles and integrated control of power coupling.

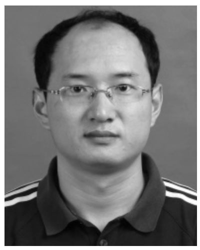

JIAN WU received the Ph.D. degree in vehicle engineering from the Nanjing University of Aeronautics and Astronautics, Nanjing, China, in 2015. He did two years research at Tsinghua University, as a Postdoctoral Researcher, from 2016 to 2018. He has been an Associate Professor with Liaocheng University, since 2018. His research interests include key technologies of intelligent driving and intelligent driving assistance system hardware in the loop technology.

DEXI WU received the B.S. degree in vehicle engineering from Liaocheng University, Shandong, China, where he is currently pursuing the master's degree in vehicle engineering. His main research interests include steering-by-wire systems and intelligent vehicle dynamics and control.

JUNDA ZHANG received the B.S. degree in vehicle engineering from Liaocheng University, Shandong, China, in 2019, where he is currently pursuing the M.S. degree. His research interests include vehicle dynamics states estimation and intelligent vehicle control.

XIANGKUN HE received the Ph.D. degree from Tsinghua University, China, in 2019. He is currently the Researcher with the Noah's Art Lab, Huawei Technology, China. His research interests mainly include vehicle motion planning and control, behavior decision-making, and deep reinforcement learning-based autonomous driving technology.